Frequency spectra of nonlinear elastic pulse-mode waves

Abraham Kadish, James A. TenCate, and Paul A. Johnson[a)]
EES-4, MS D443, Los Alamos National Laboratory, Los Alamos, New Mexico 87545

(Received 1 August 1995; revised 20 April 1996; accepted 6 May 1996)

The frequency spectrum of simple waves is used to derive a closed form analytical representation for the frequency spectrum of damped nonlinear pulses in elastic materials. The damping modification of simple wave theory provides an efficient numerical method for calculating propagating wave forms. The spectral representation, which is neither pulse length nor amplitude limited, is used to obtain estimates for parameters of the nonlinear state relation for a sandstone sample from published experimental data, and the results are compared with those of other theories. The method should have broad application to many solids.

PACS numbers: 43.25.Dc [MAB]

INTRODUCTION

Nonlinear pulse propagation experiments conducted at Los Alamos National Laboratory are directed in part at determining nonlinear state relations for elastic earth materials.[1] In one of the experimental configurations, axial compressional pulses are driven in a two meter cylindrical rod by oscillating a piezo-electric crystal at one end. Frequencies are of the order of 10 kHz and pulse times of the order of a ms. The spectrum of resulting displacements is obtained from displacement measurements made prior to the arrival of reflections from the undriven end.[2] Most of the theory in support of the program has modeled the stress–strain relation of samples assuming ideal nonlinear elasticity. Efforts to explore the effects of dissipative mechanisms and additional nonlinear contributions, (e.g., hysteresis and discrete memory) are in progress. It is likely that nonideal effects will be interpreted in terms of a departure from those of the ideal theory. In view of this, it is evident that a best possible understanding of propagation in the ideal nonlinear elastic limit is important.

In this article, a representation of the frequency spectrum for these experiments is derived that can be used to algebraically infer parameters of assumed ideal elastic stress–strain relations from measured spectral data. Although other methods have been suggested in support of these experiments,[3] attempts to determine the state relation have depended primarily on frequency domain analyses of nonlinear models which incorporate state relations with free parameters. Values of these parameters have been inferred by comparison of predicted spectral amplitudes using perturbation methods with those generated in experiments.[2,4,5] The most successful of these theories has been that of Van Den Abeele.[5] Using incremental damping corrections to undamped wave propagation similar to those of an earlier study of noise propagation in fluids,[6] very good agreement with the mode structure seen in the experiment was obtained.

In this article, propagating wave forms are calculated in the time domain by modifying undamped simple wave propagation[7] to include dissipation. The spectral representation of these waves is obtained by Fourier transform. Because the wave forms are calculated in the time domain, the evolution of the propagating pulses are easily visualized and interpreted as the results of compressions and dilations. Results of this methodology include a transparent interpretation of experiments and a more efficient and flexible numerical capability for a wider variety of pulse profiles than is achievable with other methods. The representation admits finite amplitude sources of finite pulse length.

To facilitate comparison with other theories, the representation is used in this article to analyze the spectrum of a single frequency cw source assuming a cubic approximation to the stress–strain relation. The values of the first nonlinear coefficient found here are at the upper end of the range of values found by Van Den Abeele.[5] The values of the second nonlinear coefficient found here are also contained in the range found by him, with differences in the upper and lower ranges differing by factors of 2 or less. Some general properties of propagation are illustrated numerically. A more detailed examination will appear in a separate paper.[8]

The nondissipative model is discussed in Sec. I, and the exact spectral representation for undamped wave propagation is derived in Sec. II and illustrated for a monotonal pulse in the small amplitude source approximation. In Sec. III, expressions are derived for coefficients of cubic approximations to stress–strain relations assuming weak nonlinearity in terms of spectral amplitudes. The spectral representation is corrected to include dissipation in Sec. IV, and state parameters (e.g., β and δ) are inferred from experimental data and compared to those obtained by Meegan *et al.*,[2] and Van Den Abeele. Some properties of damped wave propagation are illustrated numerically in Sec. V. We conclude with a discussion of results.

I. THE NONDISSIPATIVE MODEL

The simplest one-dimensional model for studying nondissipative compressional wave propagation from a pulsed source in an elastic medium is the first order 2×2 system

[a)]Also at Université Pierre et Marie Curie, Bureau des Mécaniques, Tour 22, 4, Place Jussieu, 75252 Paris Cedex 05, France.

consisting of the equations of continuity and force balance for the mass density per unit length, $\rho(x,t)$, and displacement velocity, $v(x,t)$. (The laboratory position coordinate is x, and time is t.) Analysis of the dynamics predicted by this model is facilitated by using Lagrangian coordinates (i.e., coordinates fixed in the material). An element undergoing displacements carries its Lagrangian coordinate, z, with it for all time. [The laboratory coordinate, x, of an element at time $t=T$ is a function of its initial position, or Lagrangian coordinate, z; $x=x(z,T)$. The displacement velocity is the partial derivative of x with respect to T.] In terms of the Lagrangian coordinate, the continuity and force balance equations are

$$\epsilon_T - v_z = 0, \quad v_T - \frac{1}{\rho^*}\,\sigma_z = 0,$$
$$\epsilon \equiv -\left(1-\frac{\rho^*}{\rho}\right) = \frac{\partial(x-z)}{\partial z}. \tag{1}$$

(If a coordinate in the unstressed bar, z, is displaced to the position, x, conservation of mass requires $\rho^*\,dz=\rho\,dx$.) Here, ρ^* is the density in the absence of stress. The elastic stress, σ, of the material is assumed to depend on space and time only via strain, ϵ. Subscripts T or z indicate partial differentiation with respect to the subscripted variable with the other held constant. [Familiar second-order wave equations for nonlinear compressional wave propagation may be obtained from Eq. (1) by elimination of variables.] If σ is a single valued function of ϵ, plasticity and damping effects are not included in this model. If the relation between stress and strain is one to one, as will be assumed in this article, the state relation may be written as either $\sigma(\epsilon)$ or $\epsilon(\sigma)$. Both functions vanish when their arguments are zero and are taken to be monotonically increasing functions of their arguments.

The system, Eq. (1), together with the state relation, yields a hyperbolic system of first-order partial differential equations for the velocity, v, and stress, σ (or strain parameter, ϵ). The local characteristic paths (or signal ''speeds'') in (z,T) space are given by[3]

$$\frac{dz}{dT} = \pm\sqrt{\sigma'(\epsilon)/\rho^*} \equiv \pm c(\epsilon), \tag{2}$$

where $\sigma'(\epsilon)=d\sigma/d\epsilon$. The space–time paths corresponding to $+c$ and $-c$ will be referred to as forward and backward propagating information paths, respectively. [$c(0)=c_0$ is the signal speed of linear wave propagation.]

When analyzing wave dynamics initiated by a pulse at one end of a bar, $z=0$, initiated at $T=0$, it is convenient to partition space–time into two regions. The first region is the collection of space–time coordinates at which time is sufficiently early that propagation at a position has not yet been affected by signal reflection from the other end of the bar. The other is its complement.

Pulse propagation experiments at Los Alamos aimed at studying nonlinear elastic properties of media analyze spectral properties of finite amplitude signal propagation in the first region. These spectra are the subject of this article. It can be shown[3,7] that for these experiments Eq. (1) predicts that in the first region (i) both v and ϵ are constant on each forward propagating path ($dz/dt=+c$) and (ii) there is a functional relation between v and ϵ:

$$v = -\int_0^{\epsilon} c(\tilde{\epsilon})\,d\tilde{\epsilon}. \tag{3}$$

Equation (3) implies that in the first region, ϵ, and therefore σ, are functions of v. Since ϵ is constant on the forward propagating paths of this region and the signal speed depends only on ϵ, each path is a straight line. The first region is, therefore, a ''simple wave region.''[7] The convergence and divergence of linear forward propagating paths in the simple wave region distort the initial pulse form, thereby altering the spectrum of the stress, strain, and velocity pulses confined to this region.

II. SPECTRA IN THE SIMPLE WAVE REGION

If $\tau(z,T)$ is the time the forward propagating path in the simple wave region passing through a point, (z,T) enters the elastic material at $z=0$ carrying information about displacements at $z=0$,

$$\tau(z,T) = T - \frac{z}{c(\epsilon(0,\tau))}. \tag{4}$$

If at z, a time-dependent pulse, $p(z,T)$, of the stress, strain, or velocity is confined to a time interval in the simple wave region, its frequency spectrum is given by its Fourier transform:

$$\begin{aligned}\widehat{p(z,\omega)} &\equiv \frac{1}{\sqrt{2\pi}}\int_{\text{pulse length}} p(z,T)\exp(-i\omega T)\,dT,\\ &= \frac{1}{i\omega\sqrt{2\pi}}\int_{\text{pulse length}} \frac{\partial p(z,T)}{\partial T}\exp(-i\omega T)\,dT,\\ &= \frac{1}{i\omega\sqrt{2\pi}}\int_{\text{initial pulse length}} \frac{dp(0,\tau)}{d\tau}\exp\{-i\omega[\tau\\ &\quad + z/c(\epsilon(0,\tau))]\}\,d\tau.\end{aligned} \tag{5}$$

Since the detector most often used in experiments is an accelerometer, $p=v$ will be employed. Using Eq. (3), Eq. (5) becomes a Fourier transform of a function of v

$$\widehat{v(z,\omega)} = \frac{1}{\sqrt{2\pi}}\int_{\text{initial pulse length}}\left\{\int_0^{v(0,\tau)}\exp\{-i\omega \times[z/c(\epsilon(\tilde{v}))]\}\,d\tilde{v}\right\}\exp(-i\omega\tau)\,d\tau. \tag{6}$$

Equation (6) may be used to determine parameters of nonlinear state relations from displacement spectra of weakly nonlinear pulses if the frequency spectrum is provided empirically.

Assuming that the pulse is weakly nonlinear, so $|v/c|\ll 1$, the expansion of the state relation is

$$\sigma(\epsilon) = (\rho^* c_0^2)\left(\epsilon + \frac{\beta}{2!}\,\epsilon^2 + \frac{\delta}{3!}\,\epsilon^3 + \cdots\right). \tag{7}$$

(The notation for the coefficients in series expansions of state relations has not been standardized: the $\beta/2!$ and $\delta/3!$ in this article are the β and δ of Meegan *et al.*[2] and the $\beta/2$ and $\delta/3$ of Van Den Abeele.[5]) Using the expansion of the state relation together with Eq. (3) yields an expansion for the strain in terms of the velocity

$$-\epsilon=\frac{v}{c_0}+\frac{\beta}{4}\left(\frac{v}{c_0}\right)^2-\frac{1}{12}(\delta-2\beta^2)\left(\frac{v}{c_0}\right)^3+\cdots .$$

Substituting this expansion in the signal speed of the exponent of the velocity transform results in an integral involving only the driving displacement velocity pulse and parameters of the Taylor series expansion of the state relation. The exponential can be expanded in a Taylor series in v/c. The result is a Fourier transform of a sum of powers of the applied displacement velocity pulse,

$$\widehat{v(z,\omega)}\equiv\frac{c_0}{\sqrt{2\pi}}\exp\left(-i\omega\frac{z}{c_0}\right)\times\int\exp(-i\omega\tau)E\left(\frac{v(0,\tau)}{c_0}\right)d\tau,$$

$$E\left(\frac{v(0,\tau)}{c_0}\right)=\left(\frac{v(0,\tau)}{c_0}\right)\left\{1-\frac{1}{2!}\left(\frac{i\omega z}{2c_0}\beta\right)\left(\frac{v(0,\tau)}{c_0}\right)+\frac{1}{3!}\left(\frac{i\omega z}{2c_0}\beta\right)\left[\left(\frac{i\omega z}{2c_0}\beta\right)+\frac{(\delta-2\beta^2)}{\beta}\right]\times\left(\frac{v(0,\tau)}{c_0}\right)^2+\cdots\right\}. \quad (8)$$

Equation (8) is the series expansion of the frequency spectrum in source amplitude for weakly nonlinear sources. The expansion may be carried out to any order, using as many terms as one desires in the expansion of the state relation. For frequencies and lead parameters (e.g., β and δ) of the state relation which leave the size of the exponential less than about one-half, the first few terms should provide a reasonably good approximation to the spectrum for the prediction and interpretation of experimental data.

If the source is predominantly multiperiod and single frequency with angular frequency, Ω, its velocity frequency spectrum may be approximated using a cw source

$$v(0,\tau)=\mu c_0\cos\Omega(\tau-\tau_0)$$

($\mu>0$ is a Mach number for the source) of infinite pulse length. The resulting frequency spectrum is a sum of Dirac δ functions centered at integer multiples of Ω (i.e., $\omega=\pm n\Omega$, $n=0,1,2,3,\ldots$). (Amplitudes of the acceleration spectrum are just $|\omega|$ times those of the velocity spectrum.) Up to and including cubic terms in v/c, one finds that amplitudes of the acceleration spectrum at z are given by

$$A(z,1\Omega)=\sqrt{2\pi}(\Omega c_0\mu)\times\sqrt{\left[1-\frac{\mu^2}{8}\left(\frac{\Omega z}{2c_0}\beta\right)^2\right]^2+\left[\frac{\mu^2}{8}\left(\frac{\Omega z}{2c_0}\beta\right)\frac{\delta-2\beta^2}{\beta}\right]^2},$$

$$A(z,2\Omega)=\sqrt{2\pi}(\Omega c_0\mu)\mu\left|\frac{\Omega z}{2c_0}\beta\right|, \quad (9)$$

$$A(z,3\Omega)=\sqrt{2\pi}(\Omega c_0\mu)\frac{9\mu^2}{8}\left|\frac{\Omega z}{2c_0}\beta\right|\times\sqrt{\left(\frac{\Omega z}{2c_0}\beta\right)^2+\left(\frac{\delta-2\beta^2}{3\beta}\right)^2}.$$

Assuming a sign for the convexity of the stress–strain relation, β is determined by the acceleration amplitude at 2Ω. The restriction for the cubic coefficient, δ, is then found either from the amplitude at 1Ω or 3Ω.

While the expression for $A(z,2\Omega)$ would be changed if the expansion were to be extended to include fourth powers of v/c, the expressions for $A(z,1\Omega)$ and $A(z,3\Omega)$ would not be. Even powers of the sine function contribute to amplitudes at even multiples of Ω, and odd powers contribute to amplitudes odd multiples of Ω.

III. COMPARISON OF SIMPLE WAVE THEORY AND EXPERIMENTAL DATA

Within the context of the model, the spectral representation given by Eq. (6) is exact in the simple wave region. Consequently, the series expansion, Eq. (8), yields the unique power series representation in source strength around zero amplitude for undamped weakly nonlinear elastic pulses. Evidently, for any finite amplitude source, if the frequencies employed or distances from the source at which data are taken are sufficiently large, successive terms in the series expansion will become comparable in magnitude, and the expressions for the state parameters obtained using familiar ''zero-amplitude'' perturbation methodology will be incorrect. The expansion remains valid, but its utilization will be more difficult.

Data from pulse propagation experiments in a Berea sandstone bar[2] are shown in Fig. 1(a) and (b).

Using the data sets and the expressions for $A(z,2\Omega)$ and $A(z,3\Omega)$,

$$\left|\frac{\Omega z}{2c_0}\beta\mu\right|^2\ll 1,$$

$$\left(\frac{\delta-2\beta^2}{\beta}\mu\right)^2=9\left[\left(\frac{8A(z,3\Omega)}{9A(z,2\Omega)}\right)^2-\left(\frac{\Omega z}{2c_0}\beta\mu\right)^2\right]. \quad (10)$$

Substituting these values in the expression for $A(z,1\Omega)$, one concludes that

$$\frac{A(z,1\Omega)}{A_{\text{linear}}(1\Omega)}\approx 1. \quad (11)$$

This is the small amplitude perturbation hypothesis in the absence of damping. However, all data sets satisfy

$$\frac{A(z,1\Omega)}{A_{\text{linear}}(1\Omega)}<\frac{1}{2}. \quad (12)$$

State relation parameters inferred from amplitudes of higher frequency modes assuming nondissipative propagation are incompatible with propagated spectral amplitudes measured at the source frequency.

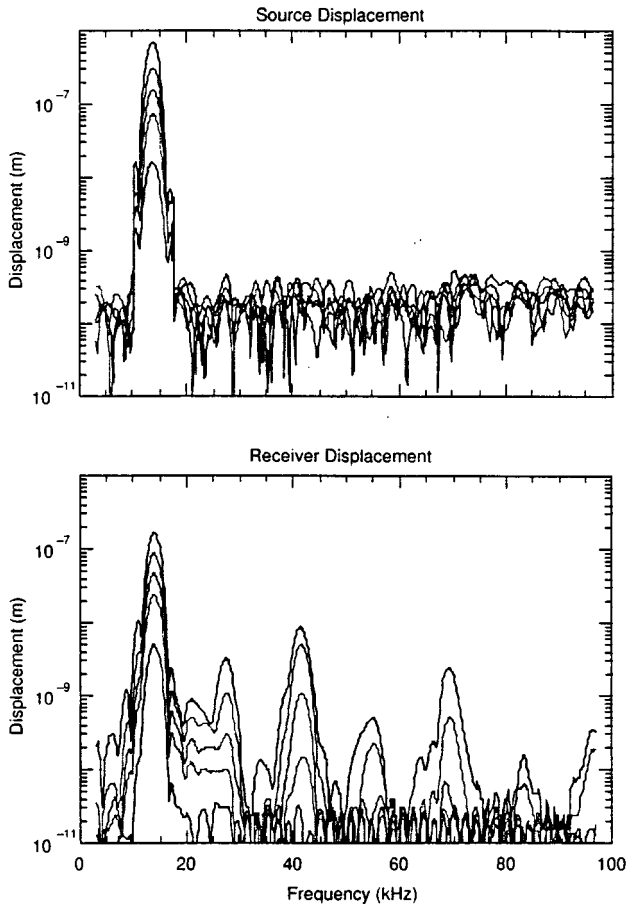

FIG. 1. (a) Source spectra measured with an optical probe for a 13.75-kHz drive; (b) spectra after the wave has propagated 0.58 m for a 13.75-kHz drive. Different curves represent different displacement amplitudes (taken from Meegan *et al.*, Ref. 2).

IV. DAMPING-CORRECTED SPECTRAL REPRESENTATION

In a recent analysis of pulse propagation experiments, Van Den Abeele[5] employed equations without dissipation to numerically propagate nonlinear waves with discrete spectra short incremental distances in a semi-infinite bar. After each incremental step, the propagated spectral amplitudes were modified assuming linear damping before being used as a source for propagation through the next incremental distance. Nonlinear evolution of the amplitudes was controlled by a small amplitude ordering assumption. In effect, a simple wave, generated by a cw source, was propagated in each interval, and the amplitudes of the propagated wave are corrected at the end of the interval assuming a phenomenological linear exponential damping. With this procedure it was found that $|\beta/2| \approx 300-500$ and $\delta/6 \approx 2(10^8-10^9)$. The range for β is much lower than that of an earlier perturbation analysis[2] that found $|\beta/2| \approx (0.5-1)10^4$, whereas the lower end of the range for δ is in agreement with the earlier suggested upper end of the range, $\delta = O(\beta^2)$.

A modification of the representation of the frequency spectrum for simple waves is now proposed in order to obtain a mathematically tractable one that includes damping effects. To obtain the representation, a linear damping of the simple wave velocity is first imposed on the simple wave signal speed paths:

$$v(z,T) = v(0,\tau)\exp(-kz). \tag{13}$$

Maintaining the simple wave relation between velocity and strain parameters, Eq. (3), and applying the damped velocity, Eq. (13), to the calculation of the signal speed path,

$$\frac{dT(z,\tau)}{dz} = \frac{1}{c(\epsilon[v(0,\tau)\exp(-kz)])},$$
$$T(z,\tau) = \tau + \int_0^z \frac{d\tilde{z}}{c(\epsilon[v(0,\tau)\exp(-k\tilde{z})])}. \tag{14}$$

The value of the velocity is carried unchanged as a function of z to the new signal speed path initiated at $(0,\tau)$.

With this procedure, damping changes the convergence and divergence of paths in what was formerly a simple wave region. Except for the uniform exponential damping of the amplitude, the assignment of velocity on each path is unchanged. Consequently, except for the uniform damping, the distribution of the spectral density is due solely to the change in the signal speed paths. Since damping with distance from the source takes the velocity to zero along each path, the paths, if continued indefinitely, would each parallel that of a linearly propagating signal. (This is illustrated in Sec. V.) However, these straight line paths, extrapolated linearly back to $z=0$, would generally not arrive there at the same times that they entered the sample. A weak amplitude signal with an approximately invariant frequency spectrum [modulo $\exp(-kz)$], different from that of the source, would propagate in z.

Because this procedure changes the geometry of the information paths from linear to curvilinear, the integrand of the Fourier transform no longer separates the time dependence of the source velocity and z in a simple way.

$$\widehat{v(z,\omega)} = \frac{e^{-kz}}{\sqrt{2\pi}(i\omega)} \int_{\text{initial pulse length}} \frac{\partial v(0,\tau)}{\partial \tau} \times \exp\left\{ -i\omega \left[\tau + \int_0^z d\tilde{z}/c(\epsilon[v(0,\tau)e^{-k\tilde{z}}]) \right] \right\} d\tau. \tag{15}$$

However, for weak nonlinearities, expansion of the state relation results in integrals of powers $\exp(-kz)$ which are easily evaluated. The resulting exponential may be expanded in a power series, as in the simple wave case, and delta functions recovered for the single frequency source.

$$\widehat{v(z,\omega)}=\frac{c_0 e^{-kz}}{\sqrt{2\pi}}\exp\left(-i\omega\frac{z}{c_0}\right)\int \exp(-i\omega\tau)E_d\left(\frac{v(0,\tau)}{c_0}\right)d\tau,$$

$$E_d\left(\frac{v(0,\tau)}{c_0}\right)=\left(\frac{v(0,\tau)}{c_0}\right)\left\{1+\frac{1}{2!}\left(\frac{i\omega z}{2c_0}\beta K\right)\left(\frac{v(0,\tau)}{c_0}\right)+\frac{1}{3!}\left(\frac{i\omega z}{2c_0}\beta K\right)\left[\left(\frac{i\omega z}{2c_0}\beta K\right)+\frac{(\delta-2\beta^2)}{\beta}C\right]\left(\frac{v(0,\tau)}{c_0}\right)^2+\cdots, \quad (16)$$

$$K\equiv\frac{1-e^{-kz}}{kz};\quad C\equiv\frac{1}{2}\left(\frac{1-e^{-2kz}}{1-e^{-kz}}\right)=\frac{1+e^{-kz}}{2}.$$

The coefficients K and C are approximately $(1-kz/2)$ and $(1+kz/2)$, respectively, if $0<kz\ll 1$. For $kz\gg 1$, their respective values are $1/kz$ and $1/2$.

Using the single frequency cw source approximation of Sec. III,

$$A_d(z,1\Omega)=\sqrt{2\pi}(\Omega c_0\mu e^{-kz})\sqrt{\left[1-\frac{\mu^2}{8}\left(\frac{\Omega z}{2c_0}\beta K\right)^2\right]^2+\left[\frac{\mu^2}{8}\left(\frac{\Omega z}{2c_0}\beta K\right)\frac{\delta-2\beta^2}{\beta}C\right]^2},$$

$$A_d(z,2\Omega)=\sqrt{2\pi}(\Omega c_0\mu e^{-kz})\mu\left|\frac{\Omega z}{2c_0}\beta K\right|, \quad (17)$$

$$A_d(z,3\Omega)=\sqrt{2\pi}(\Omega c_0\mu e^{-kz})\frac{9\mu^2}{8}\left|\frac{\Omega z}{2c_0}\beta K\right|\sqrt{\left(\frac{\Omega z}{2c_0}\beta K\right)^2+\left(\frac{\delta-2\beta^2}{3\beta}C\right)^2}.$$

The coefficient

$$A_{\text{linear},d}(\Omega)\equiv\sqrt{2\pi}(\Omega c_0\mu e^{-kz})$$

is the amplitude of the damped linearly propagating source mode. Ratios of the propagating damped modes provide two equations in two unknowns:

$$\frac{A_d(z,1\Omega)}{A_d(z,2\Omega)}=\sqrt{\left[\left(\frac{\Omega z}{2c_0}\beta K\mu\right)^{-1}-\frac{1}{8}\left(\frac{\Omega z}{2c_0}\beta K\mu\right)\right]^2+\frac{1}{64}\left(\frac{\delta-2\beta^2}{\beta}\mu C\right)^2},$$

$$\frac{A_d(z,3\Omega)}{A_d(z,2\Omega)}=\frac{9}{8}\sqrt{\left(\frac{\Omega z}{2c_0}\beta K\mu\right)^2+\frac{1}{9}\left(\frac{\delta-2\beta^2}{\beta}\mu C\right)^2}. \quad (18)$$

These relations imply

$$\left(\frac{\delta-2\beta^2}{\beta}\mu C\right)^2=9\left[\left(\frac{8A_d(z,3\Omega)}{9A_d(z,2\Omega)}\right)^2-\left(\frac{\Omega z}{2c_0}\beta K\mu\right)^2\right],$$

$$\left(\frac{\Omega z}{2c_0}\beta K\mu\right)^2=-B\pm\sqrt{B^2+8}, \quad (19)$$

$$B\equiv 4\left[\frac{1}{4}+\left(\frac{A_d(z,1\Omega)}{A_d(z,2\Omega)}\right)^2-\frac{1A_d(z,3\Omega)^2}{9A_d(z,2\Omega)}\right].$$

For the data shown in Fig. 1(a) and (b), $B>0$ and the positive square root must be chosen. With $[(\Omega z/2c_0)\beta K]^2$ and $\{[(\delta-2\beta^2)/3\beta]C\}^2$ determined from ratios of measured amplitudes, the exponential decay constant, k, may then be evaluated using any of the measured amplitudes. In particular,

$$k=\frac{1}{z}\ln\left(\frac{\sqrt{2\pi}(\Omega c_0\mu)|(\Omega z/2c_0)\beta K\mu|}{A_0(z,2\Omega)}\right). \quad (20)$$

The implied values K and C, together with those of $[(\Omega z/2c_0)\beta K)^2]$ and $\{[(\delta-2\beta^2)/3\beta]C\}^2$, then easily yield the admissible values β and δ.

The self-consistent parameters sets for the data corresponding to the two largest source strengths shown in Fig. 1(a) and (b) are

$$k\approx 1/0.23\ \text{m},\quad |\beta|\approx(1.1)10^3,\quad \delta\approx(1.6)10^9;$$
$$k\approx 1/0.27\ \text{m},\quad |\beta|\approx(1.2)10^3,\quad \delta\approx(6.9)10^9. \quad (21)$$

At $z=0.58$ m, where the data were taken, the values found for k correspond to between two and three exponential foldings of the source displacement. The linear exponential damping coefficient often employed in the frequency space description of wave propagation is $k=\omega/2Qc_0$. For the Berea sandstone sample of the Los Alamos experiment, Q is approximately 10. Using $\omega=(2\pi N)13.75$ kHz ($N=1,2,3,\ldots$) yields an exponential damping factor of $1.6N$/m. The values of k given by Eq. (20) are comparable to those used in the frequency domain when $N=2$ or 3 (i.e., 1/0.31 and 1/0.21 m).

V. NUMERICAL EXAMPLES

The results of the previous sections are now illustrated numerically using specific parametric values. The simple wave solution used here was obtained using a personal computer.

In the lossless, weakly nonlinear case, each wavelet (i.e., infinitesimal piece of the waveform) travels in space–time along characteristics [see Eq. (2)]. Figure 2(a) shows the characteristic paths for one cycle of a 13.75-kHz wave with

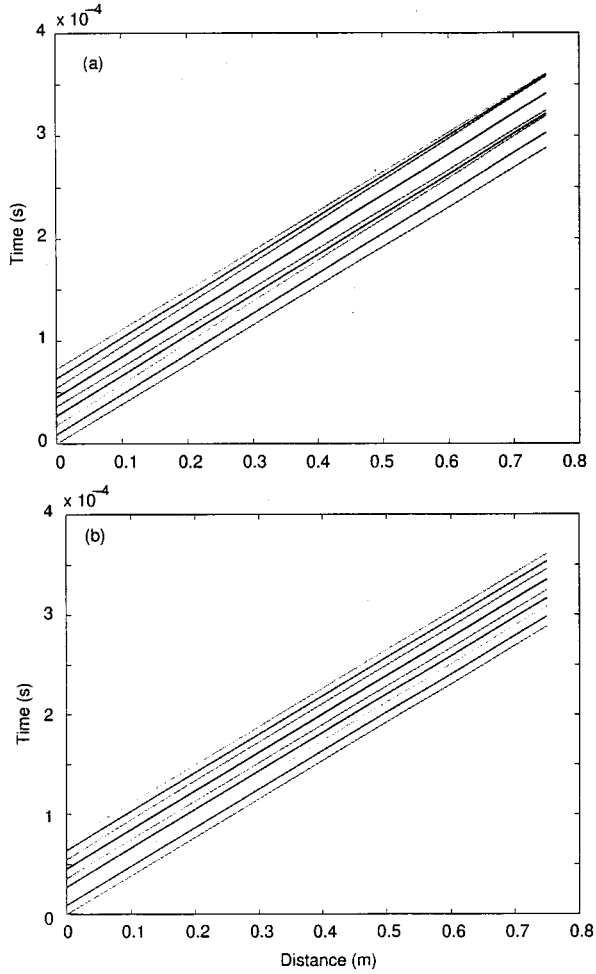

FIG. 2. Characteristics for a single cycle of a 13.75-kHz wave of displacement amplitude 5×10^{-7} m traveling in a Berea sandstone bar. Values of the nonlinear parameters β and δ used in the calculations are 10^3 and 3×10^9, respectively. Both (a) undamped and (b) damped ($k=4$/m) characteristics are shown.

displacement amplitude$=5\times10^{-7}$ m. The typical nonlinear parameters used in the calculation were $\beta=10^3$ and $\delta=3\times10^9$. Figure 2(a) shows that the wavelets near the peaks and troughs of the waveform both travel slower than those at the zeros, so the wave distorts. If the first nonlinear term (i.e., the term containing β) dominated the nonlinearity, one of these would travel faster and the other slower; the dominant contribution to the signal speed would be predominantly linear. The next nonlinear term dominates for the amplitude used in this example because of the very large value of δ. The contribution made by this term to the signal speed is predominantly cubic in the strain.

In contrast to the undamped case, Fig. 2(b) shows what happens when a damping factor $k=4/\text{m}=1/0.25$ m is applied. In the illustration, the damping is implemented numerically by taking a small, lossless distance step and applying the damping at the end of the step. The new, damped waveform is used to initiate the next lossless step and the process is repeated. The contrast between Fig. 2(a) and (b) is clear: The slopes of the paths rapidly become parallel; all parts of the wave travel with the linear signal speed, about 2.6 km/s in this case. However, the spacing between these

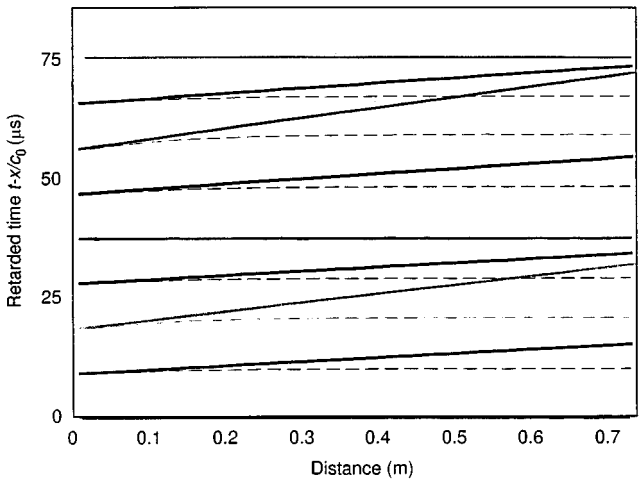

FIG. 3. Overlay of undamped and damped characteristics shown in Fig. 2. Both sets of characteristics have been rotated so that the characteristics corresponding to the zeros of the wave form (which propagate with the linear signal speed) are horizontal. Undamped characteristics are the solid lines, and damped characteristics are the dashed lines.

''nearly'' parallel paths is different from those at $z=0$. Before the damping results in approximately linear propagation, finite amplitude effects (near $z=0$) produce nonlinear divergence and convergence of signal speed paths.

To better illustrate the effect of damping, an overlay of the two sets of characteristics is shown in Fig. 3. For this plot, the characteristics shown in Fig. 2(a) and (b) were rotated so that characteristics corresponding to the zeros of the wave form (which travel at the small signal speed) are horizontal. The solid lines are the lossless characteristics, and the dashed lines are the damped characteristics. With the damping that we have chosen for this example, the waveform becomes linear (i.e., the characteristics are parallel) at only 0.2–0.3 m from the source. The damped characteristics closely follow the undamped nonlinear paths for $z<0.1$ m.

Finally, Fig. 4 shows velocity waveforms generated using the same set of parameters. Figure 4(a) shows both lossless (solid line) and damped (dashed line) waveforms after the wave has propagated 0.5 m. The difference in distortion between the two waveforms is more obvious in Fig. 4(b) where the damped waveform has been vertically expanded so that it has the same amplitude as the undamped wave form.

VI. DISCUSSION

An analytical representation, given by Eq. (15) for the frequency spectrum of nonlinearly propagating pulses in earth materials, was derived. The representation is neither pulse length nor amplitude limited. The mathematical theory underlying the derivation of the spectral representation provides a very efficient method for calculating both damped and undamped nonlinear propagating wave forms. Illustrations were shown in Sec. V.

The representation was obtained by first deriving the exact representation of the frequency spectrum for one-dimensional nonlinear pulse propagation, neglecting dissipation. Although that representation is valid (assuming undamped propagation) for any driving pulse profile, it was

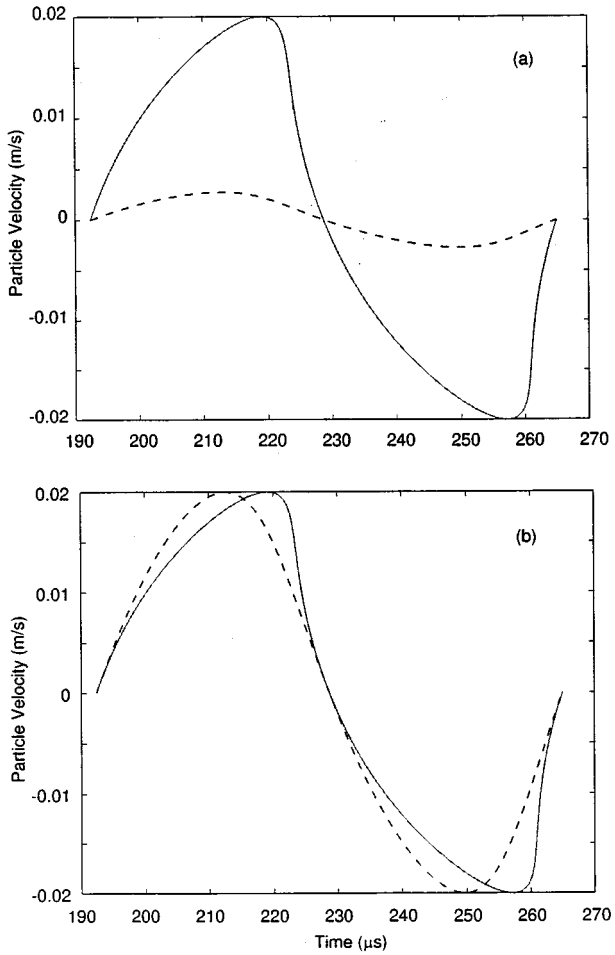

FIG. 4. (a) Velocity wave forms using the same set of parameters as those of Figs. 2 and 3. Lossless (solid lines) and damped (dashed lines) wave forms are shown after the wave has propagated a distance of 0.5 m. (b) The damped waveform has been vertically expanded to make differences between the distortions of the two waveforms more apparent.

applied in this article to a study of spectra of compressional waves generated by finite amplitude, finite pulse length sources consisting of many cycles of a single frequency. It was shown that, for typical source frequencies and amplitudes of the experiments at Los Alamos, the inclusion of dissipation in theoretical treatments is essential for even the roughest self-consistent estimates of state relation parameters from measured spectral data.

The spectral representation for the undamped simple waves was then modified to include damping effects, and the ''corrected'' spectral representation was applied to again analyze spectra from a single frequency cw pulse source. Values were obtained for the nonlinearity coefficients, β and δ, of a cubic approximation to the stress–strain relation for a Berea sandstone bar using data from the experiments. The results are given by Eqs. (21). They were compared to bounds obtained from numerical perturbation analyses. The values obtained in this article for the coefficients of both the quadratic and cubic terms are in excellent agreement with the bounds obtained from the numerical perturbation analysis of Van Den Abeele.[5]

The β's obtained in this work are more than ten times smaller than those obtained by Meegan *et al.*[2] The values of δ far exceed those required by the perturbation ordering assumption that $\delta = O(\beta^2)$. The values found imply that the spectral amplitude of the 1Ω term of the cw single frequency source is very close to that of the propagating damped linear source mode (i.e., very little energy is transferred to other modes). However, for the determination of state relation parameters, the validity of a small amplitude perturbation analysis requires both

$$\frac{1}{2}\left|\left(\frac{\omega z}{2c_0}\,\beta K\right)\left(\frac{v(0,\tau)}{c_0}\right)\right| = \frac{(1-e^{-kz})}{2}\left|\left(\frac{\omega/k}{2c_0}\,\beta\right)\left(\frac{v(0,\tau)}{c_0}\right)\right| \ll 1,$$

$$\frac{1}{3}\left|\left(\frac{\delta-2\beta^2}{\beta}\,C\right)\left(\frac{v(0,\tau)}{c_0}\right)\right| = \left(\frac{1+e^{-kz}}{6}\right)\left|\left(\frac{\delta-2\beta^2}{\beta}\right)\left(\frac{v(0,\tau)}{c_0}\right)\right| \ll 1.$$

The first inequality, which restricts $|\omega|$ For a given $z>0$, guarantees the quadratic term in the source amplitude expansion of the spectrum is smaller than the linear one. Given the first inequality, the second then guarantees that the cubic term is smaller than the quadratic one. For the parameters of these experiments, the first inequality is satisfied (it is two to three orders of magnitude smaller than unity), but the cubic term in the expansion of the spectral representation in the source amplitude is about ten times that of the quadratic term.

It is, nevertheless, interesting to note that if the calculation of the state parameters had been performed using the perturbation method, approximately the same values of k, β, and δ would have been obtained. This follows from the fact that, for the values found, the square root appearing in the expression for the spectral amplitude at 1Ω is approximately equal to unity. Thus, ignoring contributions to the 1Ω term from nonlinear terms in the source amplitude expansion gives about the same value of k. Using this value for the damping coefficient in the 2Ω term yields the same values for β. Consequently the same values for δ would be obtained from the expression for the 3Ω spectral amplitude. This approximate equivalence of methodologies is an accident attributable to the experimental data. In a system that transferred more energy from the 1Ω to the 2Ω spectral amplitude, calculated values of $|\beta|$ would be larger and would more strongly affect the calculation of the decay constant. It should be noted, in view of the relative sizes of cubic and quadratic terms in the expansion of the spectral representation, that it would not be surprising to find that assuming a linear damping and/or approximating the spectral representation by a low order polynomial in source amplitude introduces significant errors in the calculation of state relation parameters.

As a final note, it is clear from the work of others[9] that application of a classical, continuous equation of state to

earth materials may not always be reasonable. For example, hysteresis and end point memory may play a significant role in propagating waves in rocks. Consequently, multivalued equations of state may be needed for accurate modeling. However, the method presented here may have broad application to nonhysteretic materials that do not contain discrete memory and to the evaluation of nonideal effects in some earth materials. The Berea sandstone experimental results were chosen as a means of illustration only. Berea sandstone under ambient conditions almost certainly requires a multivalued equation of state in order to more precisely model its behavior.

ACKNOWLEDGMENTS

The authors would like to thank J. N. Albright and C. W. Myers for their support, and K. Van Den Abeele and K. R. McCall, R. A. Guyer, and T. J. Shankland for several informative technical exchanges. This work was supported in part by a grant from the U.S. Department of Energy Office of Energy Research and was performed under the auspices of the U.S. Department of Energy at Los Alamos National Laboratory.

[1] P. A. Johnson and P. N. J. Rasolofosaon, ''Manifestation of nonlinear elasticity in rock: convincing evidence over large frequency and strain intervals from laboratory studies,'' Nonlinear Geophys. (in review).

[2] G. D. Meegan, Jr., P. A. Johnson, R. A. Guyer, and K. R. McCall, ''Observations of nonlinear elastic wave behavior in sandstone,'' J. Acoust. Soc. Am. **94**, 3387 (1993).

[3] A. Kadish, ''Information paths and the determination of state relations from displacement measurements of elastic rods,'' J. Acoust. Soc. Am. **97**, 1489 (1995).

[4] K. R. McCall, ''Theoretical study of nonlinear elastic wave propagation,'' J. Geophys. Res. **99**, 2591 (1994).

[5] K. Van Den Abeele, ''Elastic pulsed wave propagation in media with second or higher order nonlinearity,'' J. Acoust. Soc. Am. **99**, 3334–3345 (1996).

[6] F. M. Pestorius and D. T. Blackstock, ''Propagation of finite-amplitude noise,'' in *Finite-Amplitude Wave Effects in Fluids, Proceedings of the 1973 Symposium, Copenhagen* (Dorset, Dorchester, UK, 1974), Sec. 1.3, p. 24.

[7] R. Courant and K. O. Friedrichs, *Supersonic Flow and Shock Waves* (Interscience, New York, 1948), Chap. 2, Secs. 22 and 29.

[8] J. A. TenCate, ''On the equation of state in microcracked materials,'' J. Acoust. Soc. Am. (in review).

[9] R. A. Guyer, K. R. McCall, and G. N. Boitnott, ''Hysteresis, discrete memory and nonlinear wave propagation in rock,'' Phys. Rev. Lett. **74**, 3491–3494 (1995).